Brain network interconnectivity dynamics explain metacognitive differences in listening behavior

Mohsen Alavash*, Jonas Obleser*

Department of Psychology, University of Lübeck, 23562 Lübeck, Germany

Center for Brain, Behavior, and Metabolism, University of Lübeck, 23562 Lübeck, Germany

Abstract

Complex auditory scenes pose a challenge to attentive listening, rendering listeners slower and more uncertain in their perceptual decisions. How can we explain such behaviors from the dynamics of cortical networks that pertain to control of listening behavior? We here follow up on the hypothesis that listeners' ability to flexibly adapt to challenging listening situations is supported by modular reconfiguration of auditory-control networks in a sample of N=40 participants who underwent resting-state and task functional magnetic resonance imaging (fMRI). Individual titration of a spatial selective auditory attention task maintained an average accuracy of ~70% but yielded considerable inter-individual differences in listeners' response speed and reported confidence in own decisions. Whole-brain network modularity increased from rest to task by reconfiguring auditory, cinguloopercular, and dorsal attention networks. Specifically, interconnectivity between nodes of auditory network and ciguloopercular network decreased during the task relative to resting state. Additionally, interconnectivity between nodes of dorsal attention network and cinguloopercular network increased. These interconnectivity dynamics were predictive of individual differences in response speed and confidence, the degree of which was more pronounced after incorrect judgments. Our findings uncover the behavioral relevance of functional crosstalk between auditory and attentional-control networks during metacognitive assessment of own perception in challenging listening situations and suggest two functionally dissociable cortical networked systems that shape the considerable metacognitive differences between individuals.

Keywords Adaptive listening behavior, metacognition, confidence, cinguloopercular network, dorsal attention network

**Corresponding author* Mohsen Alavash, Jonas Obleser; Maria-Goeppert-Str. 9a, 23562 Lübeck, Germany mohsen.alavash@uni-luebeck.de; jonas.obleser@uni-luebeck.de

Significance Statement

The ability to communicate in challenging listening situations varies not only objectively but also subjectively between individuals. Using fMRI and a challenging auditory task, we here show that this variability in metacognitive judgments of own listening behavior manifests in an adaptive, modular reconfiguration of brain networks. This reconfiguration involves auditory and attentional-control networks. Task-related modulations of brain interconnectvity suggest two dissociable cortical networked systems – one auditory and cinguloopercular; one auditory and dorsal-attention – that shape individual metacognitive performance during adaptive listening behavior. These findings promise new opportunities to better understand and ultimately intervene on deficits of auditory perception such as age-related sensorineural hearing loss or auditory hallucinations.

Introduction

In complex auditory scenes, attending only to what we want to hear can be a challenging task, making our listening prone to errors and uncertainties. Listening as such not only hinges on the auditory fidelity, but also requires brain networks associated with directing, switching, and maintaining auditory attention (Shinn-Cunningham, 2008; Hill and Miller, 2010). In recent years there has been growing interest in studying listening as a trait-like behavior, as individuals differ substantially in utilizing cognitive strategies to control their auditory attention (Peelle, 2017; Shinn-Cunningham, 2017; Waschke et al., 2017; Tune et al., 2021). Nevertheless, the neural underpinnings of this inter-individual variability are poorly understood.

Previous functional magnetic resonance imaging (fMRI) studies have associated auditory attention with regions overlapping with temporal and dorsal-parietal cortices (Puschmann et al., 2017; Shiell et al., 2018) as well as cinguloopercular and insular cortex in challenging listening tasks (Eckert et al., 2009; Wild et al., 2012; Erb et al., 2013; Vaden et al., 2019). In addition, as it has been reviewed elsewhere, when listeners selectively focus their auditory attention to a particular location, cortical areas overlapping with well-known visuospatial attention networks are more active as compared to when not listening (Lee et al., 2014).

In parallel, functional connectivity studies have identified large-scale brain networks involved in cognitively demanding tasks which include a cinguloopercular/insular network (Dosenbach et al., 2008; Menon and Uddin, 2010; Sadaghiani and D'Esposito, 2015), a frontoparietal network (Seeley et al., 2007; Marek and Dosenbach, 2018), and a dorsal attention network (Fox et al., 2006; Szczepanski et al., 2013). Surprisingly, whether and how these attentional control networks support adaptive listening behavior has remained somewhat understudied and incompletely understood.

The emerging field of network neuroscience provides the theoretical basis to address this question (Bassett and Sporns, 2017). Within this framework, it has been shown that most of the variance in the configuration of brain networks arise from inter-individual variability rather than task contexts (Gratton et al., 2018). Along these lines of research, our previous fMRI study provided a large-scale brain network account of adaptive listening behavior (Alavash et al., 2019). Specifically, we were able to explain individual adaptation to a challenging listening task with concurrent speech by reconfiguration of a brain network composed of auditory, cinguloopercular, and ventral attention nodes toward increased modular segregation during the task relative to resting-state baseline.

However, an often understudied and thus not explained aspect of human adaptive perception and communication lies in the subjective assessment of one's own perceptual judgments. Many neuroimaging studies of auditory cognition, including our own, have measured behavior only objectively using individuals' response accuracy (also labelled as "type I" perceptual decisions (Galvin

et al., 2003) and, sometimes, speed. Challenging listening situations naturally introduce uncertainties to individual's evaluation of own auditory perception, thus confidence in listening (secondary to listening accuracy). This subjective evaluation can be viewed as a second-order measure of listening behavior, also referred to as "type II" decision (see above ref.). Such subjective reports can vary markedly from objective measures of listening behavior (Wostmann et al., 2021).

Thus, one important question is whether and how brain network dynamics regulate listener's metacognitive assessment of own perception to support adaptive listening. Knowing the role of cinguloopercular and insular networks in listening under challenging situations, performance monitoring, and interoception (Fleming and Dolan, 2012; Barttfeld et al., 2013; Uddin, 2015; Rouault et al., 2018), it is plausible to associate these interoceptive networks with subjective evaluation of own listening performance, that is, with a variant of "metalistening". Specifically, we do not know whether and how listener's capacity of introspection to reflect on own perception relies on the interactions between distributed cortical networks.

To address this issue, we here aimed at identifying and characterizing auditory-attentional control networks and their reconfiguration in a challenging auditory task that allowed joint measurement of objective and subjective listening behavior. Thus leveraging the degree and direction of network dynamics, the present study asks two questions: (1) how are large-scale cortical networks being reconfigured to support selective listening? and (2) how can such reconfigurations explain individual differences not only in objective-perceptual, but also in subjective-metacognitive measures of listening behavior?

Results

We measured brain activity using fMRI in a sample of healthy young adults (N = 40; 18–32 y old) and constructed large-scale cortical connectivity networks (Fig. S1). This was done separately for a first 10-minute period of eyes-open resting-state measurement and for a second, ensuing 1-hour period where individuals performed an adaptive auditory task, namely selective pitch-discrimination (Fig. 1). The listening task was identical to the one used in our previous EEG study (Wöstmann et al., 2019). In brief, participants were presented with two concurrent tone sequences inside MRI scanner, one of which was always presented in front and the other in left or right in a block-wise fashion (Fig.1A). The virtual spatialization of sounds was achieved using individually selected head-related transfer functions (HRTFs; see SI Appendix for details).

On each trial, prior to tone presentation, an auditory spatial cue prompted the participants to attend to one of the tone sequences and to judge the pitch difference (increase/decrease) in the to-be-attended sequence. Listeners also reported their confidence in own decision (high/low; Fig. 1A). The pitch difference was individually titrated throughout the experiment using an adaptive tracking procedure to retain the listeners' overall accuracy at ~70% (see (Fleming et al., 2010) and (Palmer et al., 2014) for a similar titration approach in a visual perceptual task). This procedure made sure that the task was equally challenging enough as reflected in fair amount of trials with correct and incorrect responses for each listener, and in turn yielded considerable inter-individual variability in response speed and confidence across listeners (Fig. 1B).

Guided by our previous fMRI study on brain network account of spatial selective auditory attention (Alavash et al., 2019), we predicted that during the task brain networks would reconfigure toward higher functional segregation as quantified by network modularity. Importantly, we asked if a reconfiguration as such can explain inter-individual variability in listening behavior. To this end, we used (generalized) linear mixed effects models (GLMMs) to examine the influence of the

experimental conditions and brain network dynamics on listeners' single-trial behavior measured using response accuracy, speed, and confidence.

High inter-individual variability in response speed and confidence during selective pitch discrimination task

The average pitch difference between the consecutive tones (i.e., the stimulus parameter tracked per listener adaptively; Fig. 1B, Δf_0) was 0.84 semitones (± 0.69 semitones between-subject SD). As intended, the resulting accuracy (average proportion correct) was 71% (± 3.6% between-subject SD).

Notably, as illustrated in Fig.1B, listeners showed considerable inter-individual variability in their response speed (mean ± SD response speed = 1.23 ± 0.37s^{-1}; coefficient of variation = 0.3) and in their confidence (average proportion and SD of 'confident' responses = 48% ± 28%; coefficient of variation = 0.58).

Lending plausibility to the behavioral results obtained, single-trial listening behavior confirmed the beneficial effect of pitch difference on listeners' behavior, i.e., the larger the pitch difference, better the behavioral performance (GLMMs; accuracy: odds ratio (OR) = 1.42, $p < 0.001$; speed: $\beta = 0.26$, $p < 0.01$; confidence: OR = 2.97, $p < 0.001$). Listeners also showed more accurate and faster performance when the direction of the pitch change was congruent across the two tone sequences (accuracy: OR = 3.06, $p < 0.001$; speed: $\beta = 0.08$, $p < 0.01$). In addition, listeners were less confident when the to-be-attended tone sequence was presented in front compared with side (OR = 0.84, $p < 0.01$). All of these effects were very well in line with the results we found in our previous EEG study in which the stimuli during the same task were presented in free field using loudspeakers (Wöstmann et al., 2019).

Of relevance to all further brain-behavior results, the three behavioral measures proved sufficiently reliable. Only if they are sufficiently reliable, meaning that individual data on repeated tests correlate positively, any brain-behavior relation, which is the main scope here, can be interpreted in a meaningful way (Guggenmos, 2021). Using the individual data across six blocks of the task, we calculated the reliability metric Cronbach's alpha (CA) for each measure. The result indicated relatively high reliability of each behavioral measure, particularly so for response speed and confidence (accuracy: CA = 0.58, speed: CA = 0.95, confidence: CA = 0.98).

Adaptive tracking of individual accuracy at ~70% throughout the experiment allowed us to split listeners' single-trial responses into correct and incorrect judgments. Specifically, on average listeners performed 486.89 ± 69.04 trials over six blocks of task (excluding timeouts and trials with reaction time (RT) < 0.3s or RT > 3s relative to the onset of second tone). Out of these, 346.19 ± 55.89 trials were correct and 133.6 ± 32.35 were incorrect. Accordingly, to investigate the relation between response accuracy and speed or confidence across listeners, we used single-trial accuracy as a binary predictor in linear mixed effects models predicting single-trial response speed or confidence, separately. This analysis revealed that listeners were faster and more confident in their responses on correct trials as compared to incorrect trials (speed: $\beta = 0.33$, $p < 0.001$; confidence: OR = 1.89, $p < 0.001$; Fig. 1C). Important to the questions asked here, individual ability to reflect on own auditory perceptual decision varied markedly between listeners: while some listeners showed an "overconfident" behavior (i.e., high proportion of confident responses on incorrect trials), some showed an "under-confident" behavior (i.e., low proportion of confident responses on correct trials).

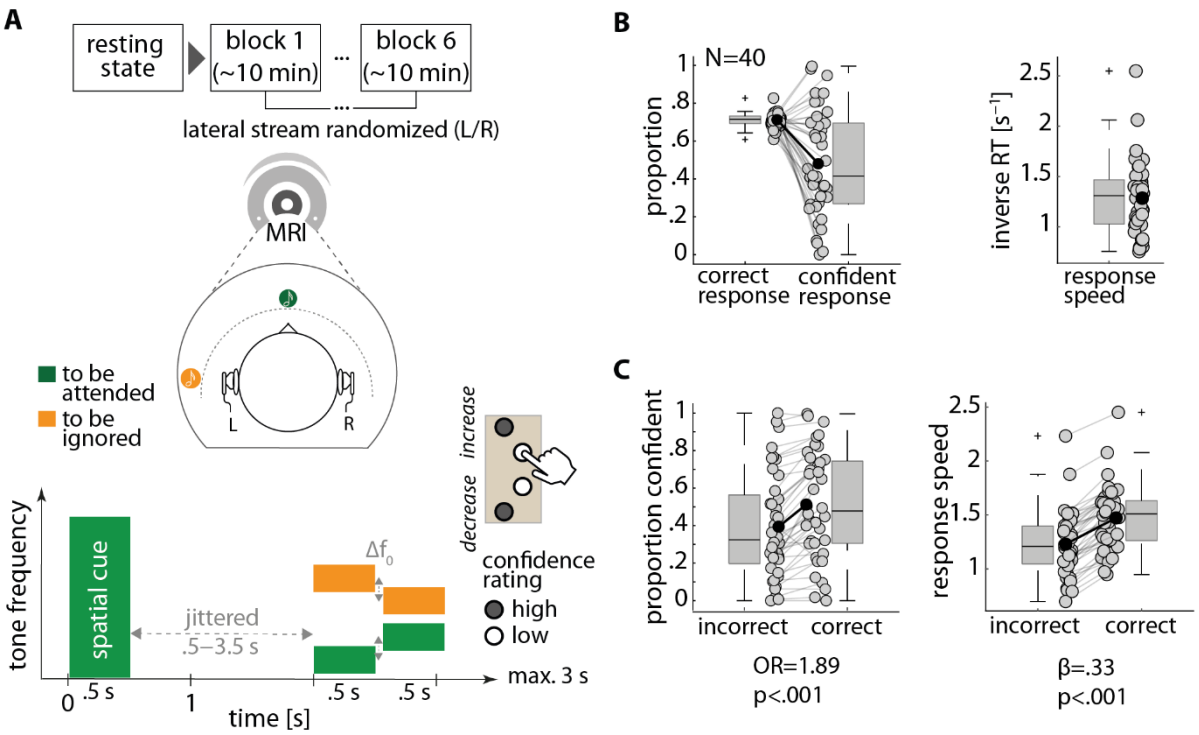

Figure 1. Listening paradigm and individuals' behavior. (A) Functional MRI experiment. Following 10-min eyes-open resting state, participants performed six blocks of purely auditory selective pitch discrimination task. During the task, two competing tone sequences were presented using in-ear headphones. The virtual spatialization of sounds was achieved using individually selected head-related transfer functions (HRTFs). One tone sequence was always presented at front and the other was switched between left and right over task blocks (left/right order randomized across participants). Each trial started by presentation of a broadband auditory cue (0–10 kHz; 0.5 s) followed by a jittered silent interval. Next, two tone sequences, each consisting of two brief (0.5 s) complex tones, were presented at different locations (front, left, or right). Fundamental frequencies of low-frequency tones within each sequence were fixed at 177 and 267 Hz. Frequencies of high-frequency tones were titrated throughout the experiment (Δf_0: tracking parameter). Participants had to judge whether the target tone sequence at the cued location had increased or decreased in pitch. Participants also reported their confidence in own decision (high: outer buttons; low: inner buttons). (B) Individuals' listening behavior. Listeners' behavior was measured both objectively and subjectively using response accuracy, speed (i.e., inverse response time; 1/RT), and confidence rating. Individuals showed considerable variability in their listening behavior, notably in response speed and confidence. (C) Prediction of single-trial response confidence and speed from accuracy. Listeners were more confident and faster in their responses on correct trials as compare to incorrect trials (linear mixed-effects models with single-trial accuracy as a binary predictor). *Box plots*. The central line indicates the median, and the bottom and top edges of the box indicate the 25th and 75th percentiles, respectively. The whiskers extend to the most extreme data points not considered outliers. The outliers are marked by '+' symbol. *Individual data*. The central solid circle indicates the mean.

Higher modularity of cortical networks during selective pitch discrimination task

Using the fMRI data, we first asked whether functional segregation of large-scale brain networks increases under listening task. Accordingly, our main analysis started by comparing functional segregation of brain networks during the task relative to rest. The degree of functional segregation can be quantified using the graph-theoretical measure known as modularity which captures the decomposability of a network into subsystems (Fig. 2A) (Rubinov and Sporns, 2010) and has been suggested to support cognitive flexibility and adaptive behaviors (Bassett et al., 2010; Alavash et al., 2015a; Bertolero et al., 2018). In the light of our previous fMRI study (Alavash et al., 2019), we expected that brain network modularity would increase during the selective pitch discrimination task relative to resting state.

Our network comparison revealed a significant increase in network modularity during the task relative to rest (permutation test; Cohen's d = 0.3, p = 0.02; Fig. 2B, left). Importantly, resting-state and listening task networks did not differ in their overall mean functional connectivity (Cohen's d = –0.01, p = 0.93). This emphasizes the importance of modular reconfiguration (i.e., change in network topology) in brain network adaptation to the current task context in contrast to a mere alteration in overall functional connectivity. This result was in good agreement with our previous study in which whole-brain network modularity increased during a dichotic listening task with concurrent speech (Alavash et al., 2019).

In an additional analysis, we investigated the correlation between resting-state and task brain connectivity and network modularity, separately. Reassuringly, both measures were positively correlated across participants (connectivity: Spearman's rho = 0.5, p < 0.01; modularity: rho = 0.61, p < 0.01), supporting the idea that state- and trait-like determinants both contribute to individuals' brain network configurations (Geerligs et al., 2015). Lending generality to all further results, we did not find any significant difference in network modularity between attend left versus attend right (permutation test; d = 0.04, p = 0.5), or left versus front (d = 0.03, p = 0.75), or right versus front (d = 0.01, p = 0.86).

We next investigated whether reconfiguration of the whole-brain networks from rest to task can account for the inter-individual variability in listening behavior (Fig. 1C). To this end, using the same linear mixed effects model that revealed the beneficial effects of the pitch difference and congruency of the tone pairs on objective and subjective measures of behavior, we tested the direct and interactive effects of brain network modularity during task in predicting listeners' behavior. By including single-trial accuracy as a binary predictor in our models we were able to additionally test the interaction between network modularity and accuracy in predicting response speed or confidence. In these models, we also included whole-brain mean connectivity as a between-subject covariate.

We found a significant main effect of network modularity in predicting single-trial response confidence (OR = 0.85, p < 0.01, log[Bayes factor(BF)] = 3.77; Fig. 2B). This result indicated that those listeners who showed higher brain network modularity during the task performed less confident. However, prediction of confidence from network modularity did not differ between correct and incorrect judgments (modularity × accuracy interaction: OR = 1.09, p = 0.15). Taken together, these results provided initial evidence that, at the whole-brain level, reconfiguration of network modules is task-relevant, as it has the potential to explain individual differences in listeners' response confidence.

The effects of pitch difference, congruency of the tone pairs, or role of the lateral stream (i.e., to-be-attended or to-be-ignored) on single-trial confidence ratings did not moderate these whole-brain

network modularity effects. Adding an interaction term between these experimental conditions and brain network modularity did not significantly improve model fit (likelihood ratio tests; pitch difference: $\chi2 = 0.54$, $p = 0.45$; congruency: $\chi2 = 0.01$, $p = 0.92$; role of the lateral stream: $\chi2 = 3.2$, $p = 0.07$). Also, the interaction between rest and task modularity did not contribute to predicting single-trial accuracy or response speed (accuracy: OR = 1.02, $p = 0.79$; speed: $\beta = -0.02$, $p = 0.35$).

Following the analysis rationale established in (Alavash et al., 2019), the following sections will explore the cortical origin of the modular reconfiguration outlined above: first, at the whole-brain level and second, at a subnetwork and nodal levels in more detail. In the final section of the results, we will illustrate how these network dynamics can explain metacognitive differences in listening behavior.

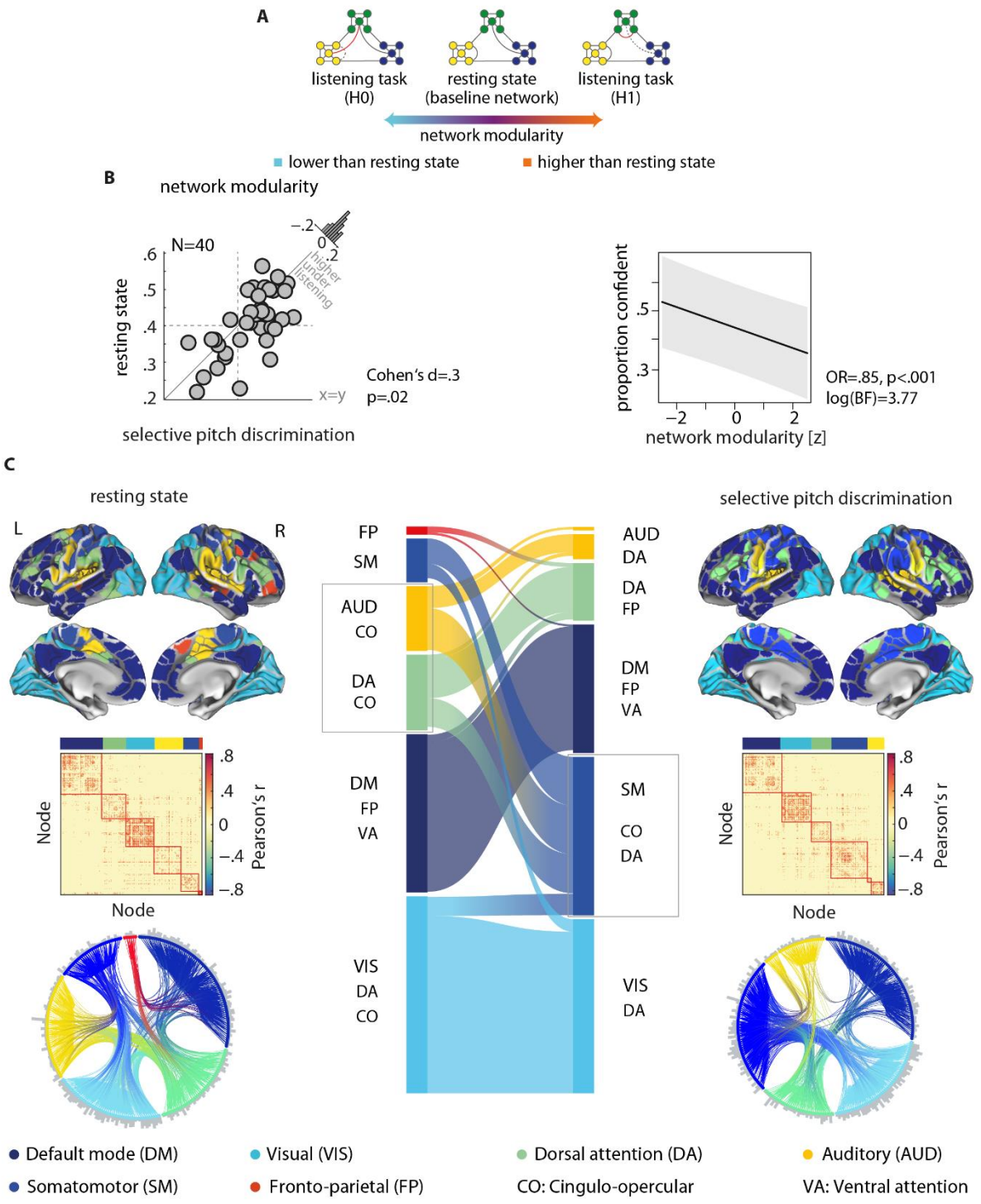

Figure 2. Reconfiguration of whole-brain network under the listening task relative to resting state. (A) Two possible network reconfigurations (i.e., left/right toy graphs compared to middle graph). Higher functional segregation is characterized by an increase in network modularity, a measure that quantifies grouping of nodes into relatively dense subsystems (here shown in distinct colors), which are sparsely interconnected. Toward higher functional segregation, the hypothetical baseline network loses the shortcut between the blue and green module (dashed link). Instead, within the green module, a new connection emerges (red link). (B) During the listening task, network modularity significantly increased (left plot), the degree of which predicted lower proportion of confident responses across listeners (right plot). Histogram show the distribution of the change (task minus rest) across all 40 participants. (C) Whole-brain resting-state network decomposed into distinct modules shown in different colors. The network modules are visualized on the cortical surface, within the functional connectivity matrix, and on the connectogram using a consistent color scheme. Modules are identified according to their node labels as in Gordon parcellation. Group-level modularity partition was obtained using graph-theoretical consensus community detection. Gray peripheral

bars around the connectograms indicate the number of connections per node. Flow diagram in the middle illustrates the reconfiguration of brain network modules from resting state (left) to the listening task (right). Modules are shown in vertical boxes with their heights corresponding to their connection densities. The streamlines illustrate how nodes belonging to a given module during resting state change their module membership under the listening task.

Reconfiguration of auditory and attentional-control networks during selective pitch discrimination task

Fig. 2C provides a comprehensive overview of group-level brain networks, functional connectivity maps, and the corresponding connectograms (circular diagrams) during resting state (Fig. 2C, Left) and during the listening task (Fig. 2C, Right). In Fig. 2, cortical regions defined based on Gordon parcellation (Gordon et al., 2016) are grouped and color coded according to their module membership determined using the graph-theoretical consensus community detection algorithm (see SI Appendix for details). When applied to the resting-state data in our sample (N = 40), the algorithm decomposed the group-averaged whole-brain network into six modules (Fig. 2C, Left). The network module with the highest number of nodes largely overlapped with the known default mode network (Fig. 2C, dark blue). Guided by our previous study (Alavash et al., 2019) our investigation was particularly focused on the module comprising mostly auditory nodes and a number of cinguloopercular nodes (Fig. 2C, yellow). For simplicity, similar to (Alavash et al., 2019) we will refer to this module as the auditory module. Additional network modules included visual (Fig. 2C, cyan), somatomotor (Fig. 2C, light blue), dorsal attention (Fig. 2C, green), and frontoparietal module (Fig. 2C, red).

Fig. 2C shows how the configuration of the whole-brain network changed from rest to task. This network flow diagram illustrates whether and how cortical nodes belonging to a given network module during resting state (Fig. 2C, Left) changed their module membership during the listening task (Fig. 2C, Right). The streamlines tell us how the nodal composition of network modules changed, indicating a functional reconfiguration. According to the streamlines, the auditory and dorsal attention modules showed the most prominent reconfiguration (Fig. 2C, yellow and green modules, respectively), while the other modules underwent only moderate reconfigurations. This reconfiguration is very well in line with the results we found in our previous study, in which N = 49 participants completed resting state followed by selective listening task with concurrent speech.

Specifically, here this reconfiguration can be summarized by a nodal "branching" of the auditory module during selective pitch discrimination (Fig. 2C, left gray box) accompanied by formation of a module comprised of cinguloopercular, somatomotor, dorsal attention, and visual nodes. Knowing the pure auditory nature of the listening task here, the less prominent changes in visual nodes deem unlikely to be behaviorally relevant to task performance. To rule this out, for our brain-behavior models, we conducted control analyses in which main predictors were derived from visual or somatomotor networks (see section *Control analyses*). Taken together, we have observed a reconfiguration of the whole-brain network that is dominated by alterations across auditory, cinguloopercular, and dorsal attention nodes.

Accordingly, we next identified the cortical origin of these network dynamics based on the underlying functional parcellation (Gordon et al., 2016). The identified subnetwork entails auditory, cinguloopercular, and dorsal attention nodes. We will refer to this large-scale cortical subnetwork collectively as the auditory attentional-control network. This subnetwork encompasses 96 nodes (of 333 whole-brain nodes). According to Fig. 2C, this subnetwork is in fact a conjunction across all auditory, cinguloopercular, and dorsal attention nodes. For the purpose of a more transparent illustration, the cortical map of the auditory attentional-control network is visualized in Fig. 3A.

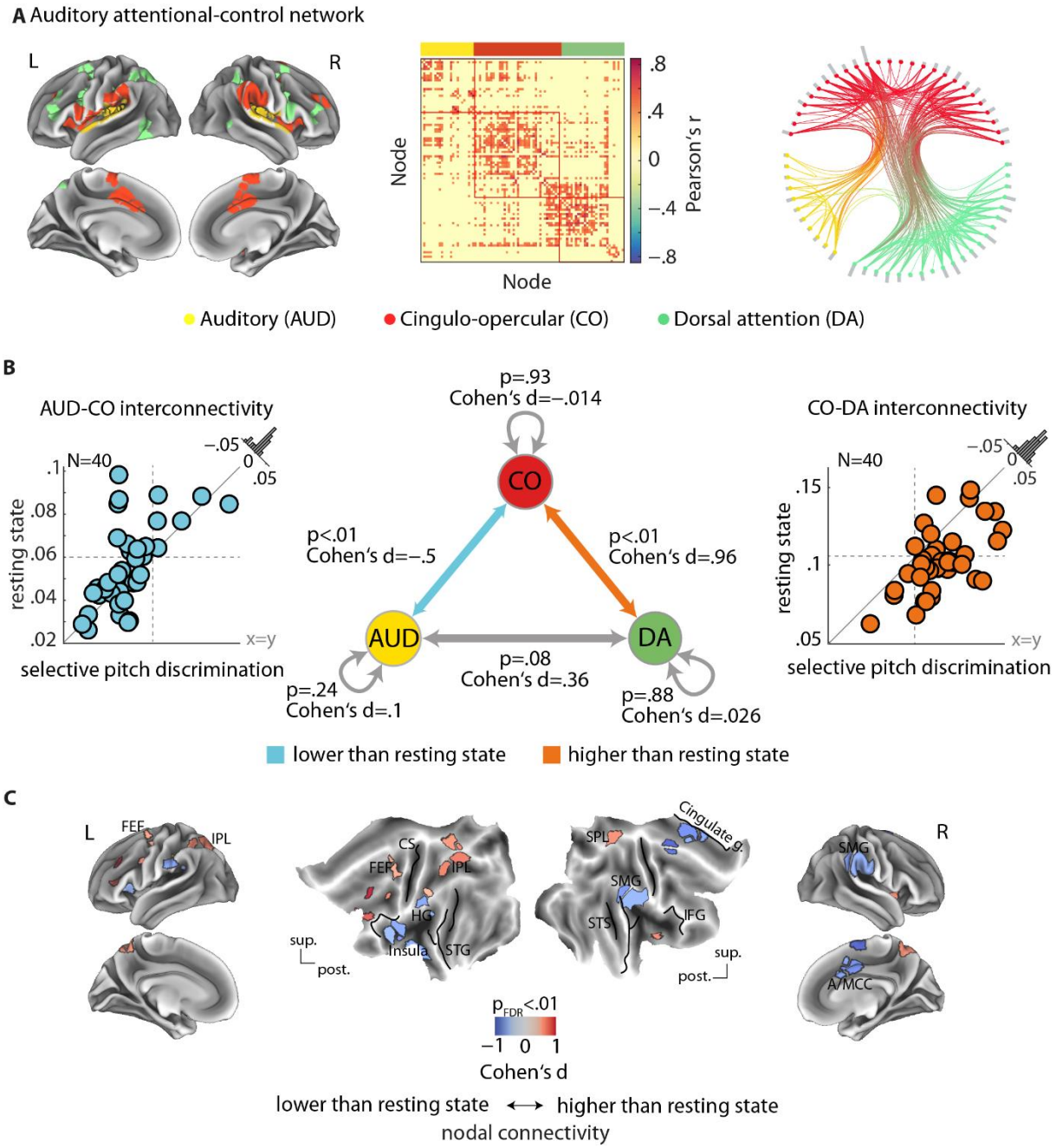

Figure 3. Modulation of connectivity across auditory and attentional-control networks. (A) The auditory attentional-control network composed of auditory (AUD), cinguloopercular (CO), and dorsal attention (DA) nodes. Nodes are identified according to their labels in Gordon parcellation. The correlation structure and connection pattern across these nodes are illustrated by group-level functional connectivity matrix and the connectogram (circular diagram), respectively. Gray peripheral bars around the connectogram indicate the number of connections per node. (B) Modulation of cinguloopercular connectivity with auditory and dorsal attention networks during the listening task. From rest to task, AUD-CO mean interconnectivity decreased (left plot), whereas CO-DA interconnectivity increased (right plot). Mean connectivity across nodes within each network or between auditory and dorsal attention networks did not change significantly (middle graph, gray arrows). Histograms show the distribution of the change (task minus rest) across all 40 participants. (C) Modulation of nodal connectivity across the auditory attentional-control network. Nodal connectivity (also known as strength) was quantified as the sum of correlation values per node. The result was compared between task and rest per node using paired permutation tests and corrected for multiple comparison across nodes (FDR correction at significance threshold 0.01). Nodes showing significant decrease in their connectivity during the listening task overlapped with bilateral supramarginal gyri (SMG), left anterior insula, and right anterior/middle cingulate cortices (A/MCC). Nodes showing significant increase in their connectivity overlapped with superior parietal/intraparietal lobule (SPL/IPL) and frontal eye fields (FEF). *CS*: central sulcus. *HG*: Heschl gyrus. *IFG*: inferior frontal gyrus. *STG/S*: superior temporal gyrus/sulcus.

Modulation of interconnectivity across the auditory attentional-control network

To uncover network dynamics underlying the modular reconfiguration of the auditory attentional-control network in adaptation to the listening task, we investigated whether and how connectivity within and between auditory, cinguloopercular, and dorsal attention nodes is modulated during the listening task relative to rest.

The result is visualized in Fig. 3B. We found two different patterns of connectivity modulation across the auditory attentional-control network. First, from rest to task, mean connectivity between auditory and cinguloopercular network (AUD-CO) was decreased significantly (Cohen's $d = -0.5$, $p < 0.01$; Fig. 3B, Left). Second, mean connectivity between cinguloopercular and dorsal attention network (CO-DA) increased significantly (Cohen's $d = 0.96$, $p < 0.01$; Fig. 3B, Right). In addition, connectivity between auditory and dorsal attention network was increased, but the degree of this modulation did not reach the significance level (Cohen's $d = 0.36$, $p = 0.08$; Fig. 3B, Bottom).

Notably, mean connectivity within auditory or cinguluopercular or dorsal attention network was not significantly different than rest (Fig. 3B, gray self-connections). This observation speaks to the potency of functional crosstalk between auditory and attentional-control networks (i.e., interconnectivity) to regulate or contribute to metacognitive aspect of listening behavior.

Interestingly, AUD-CO interconnectivity and CO-DA interconnectivity were uncorrelated across participants under both rest and task (rest: rho=–.14, p=.4, task: rho=–.03, p=.86), which suggests two dissociable large-scale networked systems shaping metacognitive performance during listening.

Next, we conducted a nodal analysis to delineate the cortical regions that drive the modulation of interconnectivity across the auditory attentional-control network. To this end, we used a simple graph-theoretical measure—namely, nodal connectivity (also known as nodal strength)—defined as the sum of each node's connection weights. Based on permutation tests to compare nodal connectivity between rest and task, we found that connectivity of mainly supramarginal gyri, anterior insular, and anterior/mid-cingulate cortices was significantly decreased during the selective pitch discrimination task relative to rest ($-1 <$ Cohen's $d < -0.53$, $p < 0.01$, false discovery rate (FDR)-corrected for multiple comparisons across nodes; Fig. 3C, blue). In addition, we found significant increase in connectivity of cortical nodes overlapping with parietal lobules and frontal eye-fields ($0.43 <$ Cohen's $d < 1$, $p < 0.01$; Fig. 3C, red).

Interconnectivity of auditory attentional-control network predicts metacognitive differences in listening behavior

As Fig. 3B shows, listeners clearly showed inter-individual variability in the degree and direction of modulation in AUD-CO and CO-DA interconnectivity. Thus, we next investigated whether these variabilities could explain inter-individual variability in listening behavior reported earlier (Fig. 1C). To this end, we tested the direct and interactive effects of individual mean interconnectivity during rest and task on single-trial response accuracy, speed, or confidence. Specifically, joint analysis of single-trial response accuracy with speed and confidence allowed investigating whether and how the interconnectivity dynamics underlie individual differences in metacognitive performance, i.e., response speed or confidence after correct/incorrect judgments. These are the same linear mixed-effects models based on which the beneficial effects of pitch difference and congruency on behavior as well as higher confidence and response speed on correct trials as compared to incorrect trials was reported earlier.

The brain-behavior relationships were tested in separate models for each AUD-CO and CO-DA network pairs. In each model, brain regressors were entered as between-subject covariates. In our models we controlled for activity level of each auditory, cinguloopercular, and dorsal attention network by including mean beta estimates derived from nodal activation analysis (Fig. S2) as additional between-subject covariates.

First, AUD-CO interconnectivity and response accuracy interacted in predicting listeners' response confidence (OR = 0.87, $p < 0.05$, log(BF) = 2.44; Fig 4A): Across listeners, lower AUD-CO interconnectivity predicted less confidence in own perceptual judgments (main effect of AUD-CO interconnectivity on response confidence; OR = 1.13, $p < 0.001$), but this relationship was more pronounced following incorrect as compared to correct judgments (incorrect: OR = 1.25, correct: OR = 1.09). Related, lower AUD-CO interconnectivity overall predicted slower decisions during the task ($\beta = 0.08$, $p < 0.001$, log(BF) = 13.73) the degree of which did not differ between correct/incorrect judgments (interaction term: $\beta = -0.02$, $p = 0.67$).

Second, dynamics of CO-DA interconnectivity predicted individual differences in response confidence (Fig. 4B). Specifically, we found a significant interaction between CO-DA interconnectivity and response accuracy in predicting listeners' confidence (OR = 1.14, $p < 0.05$, log(BF) = 1.53; Fig. 4B): Across listeners, higher CO-DA interconnectivity predicted less confident behavior (main effect of CO-DA interconnectivity on response confidence: OR = 0.88, $p < 0.001$). This negative relationship was also more pronounced after incorrect judgments as compared to correct judgments (incorrect: OR = 0.8, correct: OR = 0.96).

Having uncovered the link between interconnectivity dynamics of the auditory attentional-control network and individual listening behavior, we next asked which cortical regions within this network can explain metacognitive differences in listening behavior. To this aim, for each node within the auditory attentional-control network we estimated the linear mixed-effects model that revealed the brain-behavior relations reported above. In these models, the predictor that represented mean interconnectivity of the network pairs (i.e., AUD-CO or CO-DA mean interconnectivity) was replaced with nodal connectivity of each region within the auditory attentional-control network. Accordingly, the p-values obtained for the interaction between nodal connectivity and response accuracy were corrected for multiple comparisons across nodes (FDR correction at significance threshold 0.01).

We found significant interactions between response accuracy and nodal connectivity of brain regions overlapping with auditory/insular, superior parietal, and middle cingulate cortices (Fig. 5A). The direction of these interactions were different between two sets of nodes. Specifically, cortical nodes at the vicinity of Heschl gyrus, anterior insula, and middle cingulate cortex (MCC) showed odds ratios smaller than one, suggesting a relation between their nodal connectivity and listeners' response confidence in the direction consistent with the effect found based on mean AUD-CO interconnectivity (Fig. 5A, blue regions). In contrast, cortical nodes at the vicinity of bilateral superior parietal lobule and left inferior parietal lobule (IPL) showed odds ratios larger than one, suggesting a relationship between their nodal connectivity and listeners' response confidence in the direction consistent with the effect found based on mean CO-DA interconnectivity (Fig. 5A, red regions).

To illustrate, interactions found in left IPL and right MCC are shown in Fig 5B. Consistent with the results obtained based on mean AUD-CO interconnectivity (Fig. 4A), we found a significant interaction between nodal connectivity of right MCC and response accuracy in predicting listeners' confidence (OR = 0.76, $p < 0.001$, log(BF) = 16.4; Fig 5B, left). This result indicates that, across listeners lower nodal connectivity of right MCC predicted less confident responses, but this relationship was specific to incorrect judgments (incorrect: OR = 1.2; correct: OR = 0.97). In addition, in line with the

results obtained based on mean CO-DA interconnectivity (Fig. 4B), we found a significant interaction between nodal connectivity of left IPL and response accuracy in predicting listeners' confidence (OR = 1.35, p < 0.001, log(BF) = 17.1; Fig 5B, right): Across listeners higher nodal connectivity of IPL predicted less confident responses, but this relationship was specific to incorrect judgments as compared to correct judgments (incorrect: OR = 0.77, correct: OR = 0.98)

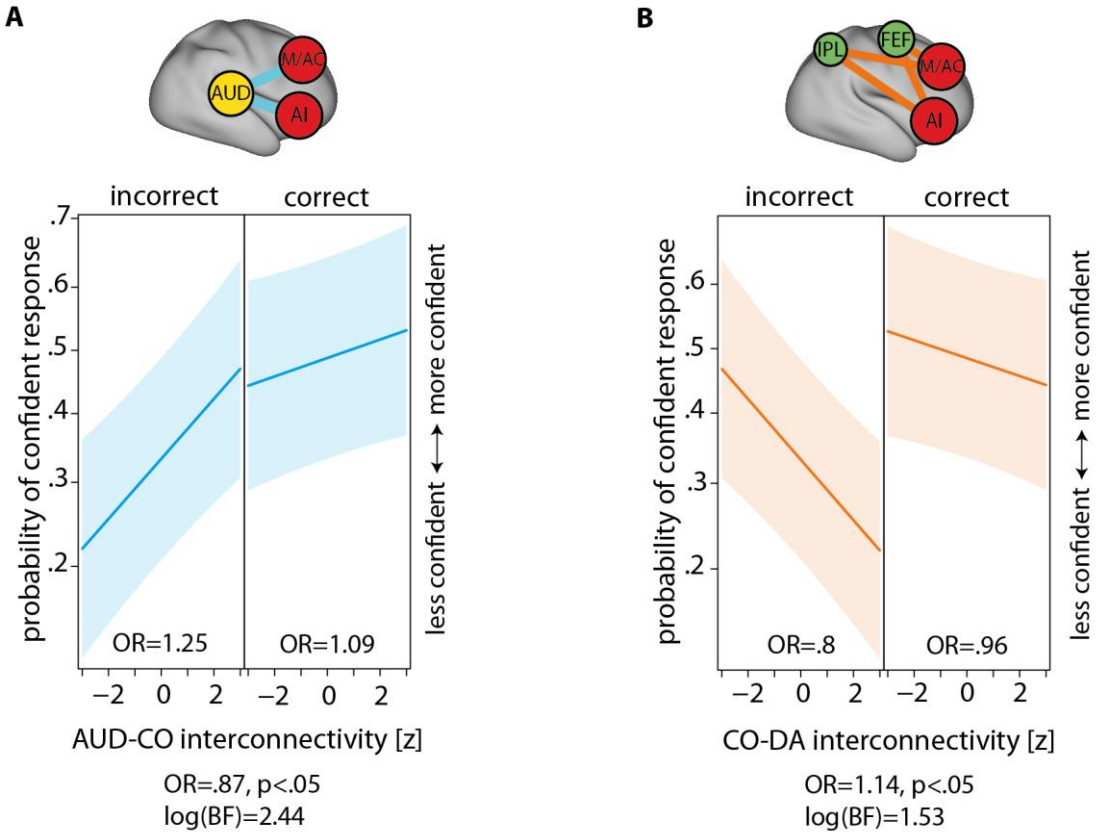

Figure 4. Prediction of individual listening confidence from interconnectivity dynamics of auditory attentional-control network (A) Prediction of single-trial response confidence from mean AUD-CO interconnectivity during the selective pitch discrimination task. Across listeners, lower AUD-CO interconnectivity predicted less confident responses during the task, the degree of which was more pronounced under incorrect judgments as compared to correct judgments. (B) Prediction of single-trial response confidence from mean CO-DA interconnectivity. Across listeners, higher CO-DA interconnectivity predicted less confident responses during the task, the degree of which was stronger under incorrect judgments as compared to correct judgments. Experimental variables including single-trial pitch differences, congruency of tone pairs, and location of spatial cue have been accounted for in the models. Shaded areas show two-sided parametric 95% CI. *OR*: odds ratio parameter estimate from generalized linear mixed-effects model. *AI*: Anterior insula. *FEF*: Frontal eye-fields. *IPL*: Inferior parietal lobule. *M/AC*: Mid-/anterior cingulate.

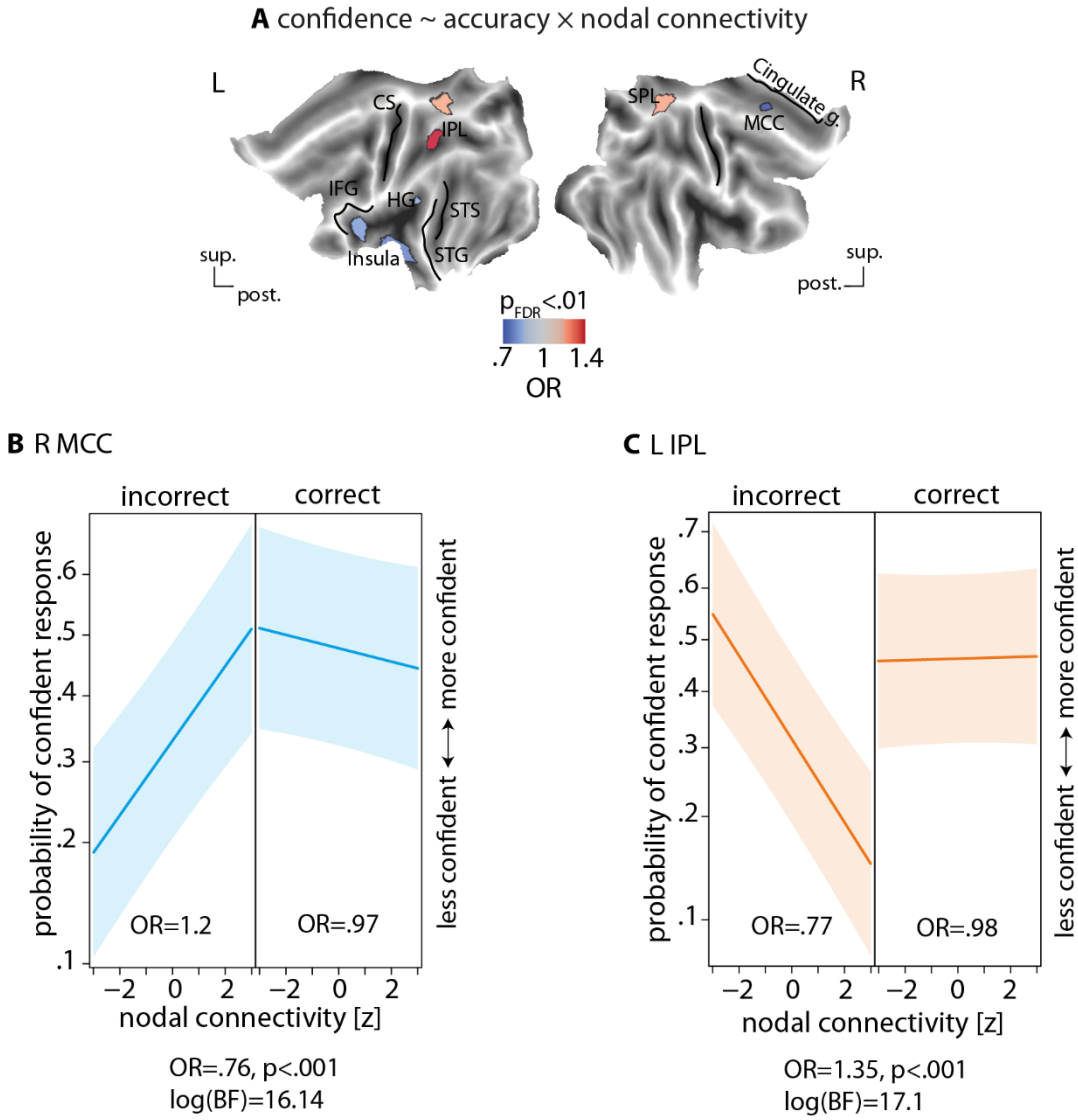

Figure 5. Prediction of individual listening confidence from nodal connectivity of the auditory attentional-control network. (A) Interaction between response accuracy and nodal connectivity in predicting single-trial confidence using generalized linear mixed effects models. Experimental variables including single-trial pitch differences, congruency of tone pairs, and location of spatial cue have been accounted for in the models. The models were tested for each node of the auditory attentional-control network. The p-values obtained for the interaction term were corrected for multiple comparisons across nodes (FDR correction at significance threshold 0.01). Two sets of nodes showed significant interactions: regions at the vicinity of Heschl gyrus (HG), anterior insular (AI), and middle cingulate cortex (MCC) showed odds ratios smaller than one (suggesting a more positive slope under incorrect than correct judgments), and regions overlapping with superior/inferior parietal lobules (SPL/IPL) showed odds ratios larger than one (suggesting a more negative slope under incorrect than correct judgments). (B) To illustrate, resolving the interaction found at right MCC indicated that lower connectivity of this node predicted lower confidence following incorrect judgments. (C) Resolving the interaction found at left IPL indicated that higher connectivity of this node predicted lower confidence following incorrect trials. Shaded areas show two-sided parametric 95% CI. *OR*: odds ratio parameter estimate from generalized linear mixed-effects model. *CS*: central sulcus. *HG*: Heschl gyrus. *IFG*: inferior frontal gyrus. *STG/S*: superior temporal gyrus/sulcus.

Control analysis: Can activity or connectivity of other networks predict listeners' behavior?

Our findings illustrate that dynamics of interconnectivity across the auditory attentional-control network could partly explain individual differences in subjective listening behavior. These dynamics were expressed as modulation of mean connectivity between network pairs defined using average Pearson correlations, a commonly used measure of functional connectivity. Accordingly, one question is, in how far the brain-behavior relations observed here are driven by changes in cortical activity level rather than changes in correlation strength. In addition, from rest to task, somatomotor and visual networks also underwent a moderate reconfiguration (Fig. 2C). Thus, another question is whether interconnectivity with somatomotor or visual network can predict listeners' behavior. Therefore, we conducted a set of control analyses to ensure that the brain-behavior findings are not trivial.

First, all of the brain-behavior models have been adjusted for individual mean cortical activity of each auditory, cinguloopercular, and dorsal attention network by including between-subject covariates of mean beta estimates derived from activation analysis (Fig. S2). Also, none of these potential confound predictors on behavior proved significant (Table S1A).

Second, we tested additional brain-behavior models in which the connectivity regressors were defined based on interconnectivity between each somatomotor or visual network with auditory, cingulopercular, or dorsal attention network. Identical to our main analysis, these models were tested separately for each network pair in predicting single-trial response confidence. The results are provided in Table S1B. We only found a significant interaction between response accuracy and interconnectivty of somatomotor and auditory networks in predicting listeners' response confidence ($OR = 0.86$, $p < 0.01$). This result indicates that lower AUD-SM interconnectivty predicted lower response confidence on incorrect trials, similar to the results obtained based on AUD-CO interconnectivity.

Discussion

The main goal of our study was to explain inter-individual variability in subjective aspect listening behavior from dynamics of cortical networks pertaining to audition and cognitive control. Importantly, we experimentally controlled and assessed listening behavior at the objective level using response accuracy or speed, but also let the listeners to subjectively reflect on their own auditory perceptual decisions by reporting their response confidence, and focused on the large variability in this metacognitive aspect of listening behavior.

First, by studying modular reconfiguration of brain networks from resting state to the selective pitch discrimination task, we identified the large-scale auditory attentional-control network. Next, across this network and on individual level, we found that performing the task modulated the interconnectivity between cinguloopercular and each auditory and dorsal attention network: while auditory-cinguloopercular interconnectivity significantly decreased, we found a significant increase in interconnectivity between cinguloopercular and dorsal attention network. The results obtained from brain-behavior linear mixed-effects models supported the functional significance of these interconnectivity dynamics.

In sum, these results suggest that lower AUD-CO interconnectivity and higher CO-DA interconnectivity predicted lower response confidence following incorrect judgments, thus supporting listeners' self-evaluation of own auditory perceptual decisions.

Metacognitive facets of adaptive listening behavior

The selective listening paradigm used in the present study allowed listeners to judge the direction of pith change in a to-be-attended auditory object clearly above chance (accuracy of ~70%) but left them uncertain about their own selective perceptual decisions, as reflected in an overall response confidence of around ~50%. Across listeners, the subjective assessment of own listening performance varied considerably, and so did listeners' response speed.

Accordingly, our listening paradigm illustrates a situation where each listener's first-order performance was high, but awareness about own perception varied considerably across listeners. This highlights an important dimension to the study of adaptive listening behavior which can be formalized within the scope of metacognition as "metacognitive performance", defined as the ability to introspect about the correctness of own thoughts and actions (Fleming et al., 2012a).

While such individual differences have been related to differences in brain structure and function more broadly before (Ais et al., 2016), our findings suggest that this variability is attributed to individual differences in interconnectivity dynamics of two cortical networked systems, as discussed below.

Interconnectivity of auditory and cinguloopercular networks communicates perceptual decision confidence during listening

Our first main finding was that lower connectivity between auditory and cinguloopercular network predicted slower and less confident responses during the listening task, the latter link being more pronounced for incorrect judgments (Fig. 4A). This result is in line with the increase in network modularity (equivalently, functional segregation) observed on the whole-brain level, and in particular the prediction of less confident responses from higher functional segregation of brain networks (Fig. 2B).

Previous fMRI activation studies have consistently shown that cinguloopercular activity is predictive of word recognition during speech-in-noise experiments (Vaden et al., 2013; Eckert et al., 2016; Vaden et al., 2019). Recently, using a perceptual decision-making model, it has been shown that cinguloopercular activity contributes to criteria adjustments to optimize speech recognition performance (Vaden et al., 2022). In parallel, visual studies have shown that cinguloopercular network displays sustained activity during perceptual processing (Sestieri et al., 2014), with its activity level relating to the speed of stimulus detection (Coste and Kleinschmidt, 2016). These findings can be interpreted in the light of the proposed role for cinguloopercular cortex in performance monitoring, and more generally, adaptive control (Dosenbach et al., 2008; Power and Petersen, 2013; Neta et al., 2014; Neta et al., 2017).

Interestingly, previous work on neural correlates of metacognition during decision-making behavior support the role of frontal brain areas in subjective sense of decision confidence (Vaccaro and Fleming, 2018). Specifically, studies have found that explicit confidence estimates are tracked in cortical areas including medial/rostrolateral prefrontal cortex (De Martino et al., 2013; Hebart et al., 2016), and dorsal anterior cingulate cortex (Fleming et al., 2012b; Fleming et al., 2014). Additionally, it has been shown that medial prefrontal cortex is linked to inter- and intra-individual variation in explicit confidence estimates (Bang and Fleming, 2018). Direct evidence comes from an animal study in which authors identified the orbitofrontal cortex to be involved in confidence based behaviors (Kepecs et al., 2008). Thus, evaluation of own decision confidence during adaptive behaviors seems to critically rely on neural computations implemented across cingulate and prefrontal cortices. In our

data, this is supported by a direct link between connectivity of a node within the right middle cingulate cortex and listeners' response confidence on incorrect trials (Fig. 5B).

Collectively, the functional overlap between cinguloopercular network being involved in adaptive control and frontal cortical areas representing decision confidence fits well with the idea of a domain-general role of cinguloopercular network in neural representation of metacognitive performance (Baird et al., 2013; Rouault et al., 2018; Rouault et al., 2023). Accordingly, one possible network mechanism underlying our finding could be that, cinguloopercular nodes detect, communicate, and integrate uncertainty into decision process according to ones' listening goal (cf. (Gordon et al., 2018)). Arguably, in our data, lower AUD-CO connectivity represent listeners lower confidence in own (incorrect) decisions and delayed responses, and thus individual metacognitive ability to reflect on own decision introspectively.

Interconnectivity of cinguloopercular and dorsal attention networks accounts for metacognitive performance during selective listening

As s second main finding, higher interconnectivity between cinguloopercular and dorsal attention networks predicted listeners' lower confidence during the selective pitch discrimination task, particularly so after incorrect judgments (Fig. 4B). Selective attention, especially in visual and spatial domains, is known to recruit dorsal attention network (Corbetta et al., 2008; Petersen and Posner, 2012; Posner, 2012; Vossel et al., 2014). Neuroimaging studies have shown that spatial auditory attention recruits some of the same cortical regions as visuospatial attention (Lee et al., 2014). Activation analysis of our data indeed supports the involvement of dorsal attention nodes in selective processing of the concurrent tones (Fig. S2D). In addition, it has been shown that cinguloopercular network is flexibly linked with dorsal attention network during visuospatial or memory search, respectively, consistent with the characterization of the cinguloopercular network as a domain-general task-control system (Sestieri et al., 2014). Studies in non-human animals have also associated the canonical nodes of dorsal attention network, namely inferior parietal sulcus and supplementary frontal eye fields, to metacognitive performance during visual-spatial tasks (Kiani and Shadlen, 2009; Middlebrooks and Sommer, 2012).

Our findings add to the growing understanding of the cortical substrate of spatial selective auditory attention by illustrating that the functional crosstalk between cinguloopercular and dorsal attention network is behaviorally relevant to selective listening to the extent that it could partly explain individual differences in metacognition during listening behavior. Our nodal analysis illustrates a direct link between connectivity of parietal regions and listeners' metacognitive ability to evaluate own perception (Fig. 5B).

In comparison to the previous work, our present study is unique in two important aspects. First, the present task was neither a word recognition task (as in previous speech-in-noise experiments) nor a categorical perceptual decision-making task (e.g., absence/presence of tone). Our task challenged the listeners to flexibly switch and maintain auditory attention on a trial-by-trial basis, and meanwhile to monitor own perception and report their decision confidence accordingly at the end of each trial. As such, the task design allowed joint analysis of objective and subjective behavior during adaptive listening. To our knowledge, this is the first study that casts the problem of adaptive listening behavior into the flourishing framework of metacognition in perceptual decision-making.

Second, previous studies on metacognition or uncertainty often claim correlations between brain regional activity and some latent state of uncertainty estimated using computational models in the context of perceptual (often visual) tasks (i.e., the read out of uncertainty from neural activity) and find unitary correlate (or neural code) of decision uncertainty in early sensory areas or higher-

order cortical areas that track confidence ((Walker et al., 2023)). In the present study instead of reducing the problem of perceptual decision-making during adaptive listening down to its local computational primitives, we took a connectionist view and investigated the source of individual differences in metalistening in auditory and higher-order attentional-control networks. This allowed us to find system-level interactions between brain networks that could explain metacognitive differences in adaptive listening behavior.

Limitations and future directions

Our study attempts to fill the knowledge gap on cortical substrate of individual differences in adaptive listening behavior by studying the listening brain within the functional segregation and integration framework (Power et al., 2011). We showed that during selective pitch discrimination functional segregation of whole-brain network increased, a reconfiguration that involved the auditory attentional-control network. The interconnectivity within this network was significantly modulated by task, the degree of which predicted individual differences in listening confidence. This suggests a potential role of network hubs within this network in guiding individuals' metalistening (cf. (Gratton et al., 2017)). Indeed, it has been previously suggested that control networks do not function in isolation but rather display context-dependent dynamic interactions amongst each other in support of adaptive behaviors (Menon and D'Esposito, 2022).

Another important question is the neurophysiological basis of individual differences in metacognition during listening. Previous work from our lab provide important insights into how dynamics of low-frequency neural oscillations underlie individual differences in objective measures of selective listening behavior (Alavash et al., 2017; Wöstmann et al., 2019; Alavash et al., 2021; Tune et al., 2021). Recent studies investigating the neural correlates of metacognitive performance during perceptual decision-making suggest a link between pre-stimulus neural activity in alpha frequency band (8–12 Hz) and decision confidence (Kayser et al., 2016; Wostmann et al., 2019). Knowing the previously proposed associations between modulations in alpha oscillations and activity of cinguloopercular and dorsal attention networks (Sadaghiani and Kleinschmidt, 2016) one prediction is that alpha oscillations organize the interconnectivity dynamics found in the present study. This understanding could be best obtained using simultaneous EEG-fMRI.

Finally, the present study holds important clinical implications. Age-related hearing loss often deteriorates neural and behavioral implementation of auditory selective attention, the degree of which varies across listeners (Dai et al., 2018; Tune et al., 2021). Objective measures of listening behavior, however, do not reveal the full spectrum of problems that the hearing impaired experiences in challenging listening situations (Wostmann et al., 2021). To understand, predict, or compensate this deficit at the individual level, it is essential to find neural markers of subjective and objective measures of selective listening. It is entirely uncharted how hearing loss might affect the capacity to monitor or calibrate own listening behavior (i.e., metacognition of listening or "meta-listening"). Our study suggests interareal connectivity of brain networks as a first approximation for addressing this question at both behavioral and brain level (Waters et al., 2012).

Materials and Methods

Participants

Forty-five participants were invited to take part in the study. All participants were right-handed (assessed by a translated version of the Edinburgh Handedness Inventory (Oldfield, 1971)), had normal or corrected-to-normal vision, and all had normal hearing (assessed using pure tone audiometry (PTA); left-right average PTA across frequencies .025-8KHZ < 25 dbHL). None of the participants had any history of neurological or psychiatric disorders. Five participants were excluded as their data did not fulfill the criteria used to assess the quality of fMRI images (see section *FMRI data acquisition and preprocessing* below). Accordingly, 40 participants were included in the main analysis (age range = 18-32 years, median age = 23, 13 males). All procedures were in accordance with the Declaration of Helsinki and approved by the local ethics committee of the University of Lübeck. All participants gave written informed consent and were financially compensated (10€/h).

Procedure

Each imaging session consisted of seven fMRI runs (Fig. 1A): eyes-open resting state (~10 min) followed by six runs in which participants performed an adaptive selective pitch discrimination task (~10 min each) (SI Appendix has a detailed description of the stimuli and task). During each resting state and each run of the listening task, 610 and 550 functional volumes were acquired, respectively. A structural scan (~5 min) was acquired at the end of the imaging session (SI Appendix has MRI acquisition parameters). Before functional and structural imaging, outside MRI room, each participant completed a screening procedure used to assess handedness, a shortened version of the Spatial, Speech and Hearing Quality Scale (SSQ; (Gatehouse and Noble, 2004))., as well as complete pure tone and speech-in-noise audiometry in free field in a sound-attenuated cabin.

FMRI analysis

An overview of the steps undertaken to preprocess and analyze the fMRI data is provided in Fig. S1. Volumetric images acquired from each participant were converted from DICOM format to standard BIDS format (Gorgolewski et al., 2016) using HeuDiConv (Halchenko, 2018). The result of this conversion was used as the input for preprocessing using fMRIPrep (Esteban et al., 2019). At this step, minimal preprocessing was applied to the data using standard fMRIPrep procedure (see SI Appendix text for details). In addition, image quality measures were extracted from outputs of DICOM-to-BIDS conversion using MRIQC tool (Esteban et al., 2017). To control the quality of the data, we used the criteria identical to (Faskowitz et al., 2020). Specifically, functional data were excluded if more than 25% of the frames exceeded 0.2-mm framewise displacement (Parkes et al., 2018), or if marked as an outlier (exceeding 1.5×interquartile range (IQR) in the adverse direction) in more than half of the following seven image quality metrics (calculated within datasets, across all functional acquisitions): dvars, tsnr, fd mean, aor, aqi, snr and efc (see MRIQC documentation for definitions). Accordingly, five data sets and two runs of two participants were excluded from the main analysis.

Cortical parcellation. As in our previous study (Alavash et al., 2019) cortical nodes were defined using a previously established functional parcellation (Gordon et al., 2016), which has shown relatively higher accuracy compared with other parcellations (Arslan et al., 2017). This parcellation is based on surface-based resting-state functional connectivity boundary maps and encompasses 333 cortical areas. To obtain Gordon333 parcellation in subject space, we used the maTT toolbox as in (Faskowitz et al., 2020). In brief, for each participant a Gaussian classifier surface atlas was used in combination with FreeSurfer's mris_ca_label function to transfer the group average atlas to subject

space based on individual surface curvature and sulcal patterns. This method rendered a T1w space volume for each participant. For use with functional data, the parcellation was resampled to 2-mm T1w space.

Nuisance regression. To minimize the effects of spurious temporal correlations induced by physiological and movement artifacts, a nuisance regression procedure was implemented using the fmri-2-mqt toolbox as in (Faskowitz et al., 2020). In this procedure, each pre-processed BOLD image is linearly de-trended, confound regressed and standardized. The confound regression employed was identical to our previous study (Alavash et al., 2019) and included six motion estimates and their first-order derivatives, time series of the mean cerebrospinal fluid, and mean white matter signal. Note that global signal was not regressed out from the regional time series, as it is still an open question in the field what global signal regression in fact regresses out (Murphy and Fox, 2016; Power et al., 2017). Importantly, our main results point to the reconfiguration of an auditory attentional-control network, which does not overlap with the mainly sensorimotor disruption map of the global signal (Power et al., 2017). After pre-processing and nuisance regression, residual mean BOLD time series at each node were recovered. This processing was performed for both resting-state and listening-task data. To allow for signal equilibration, the first 10 volumes of resting state and each run of the listening task were removed.

Functional connectivity. Residual time series were band-pass filtered by means of maximum overlap discrete wavelet transform (Daubechies wavelet of length eight as implemented in waveslim R package), and the results of the filtering within the range of 0.06–0.12 Hz (wavelet scale three) were used for additional analyses, identical to our previous work (Alavash et al., 2019). It has been previously documented that the behavioral correlates of the functional connectome are best observed by analyzing low-frequency large-scale brain networks (Zhang et al., 2016). The use of wavelet scale three was motivated by previous work showing that behavior during cognitive tasks predominately correlated with changes in functional connectivity in the same frequency range (Alavash et al., 2015b; Alavash et al., 2018). To obtain a measure of association between each pair of cortical regions, Pearson correlations between wavelet coefficients were computed, which resulted in one 333×333 correlation matrix per participant for each resting state and run of the listening task (Fig. S1).

Network analysis. Brain graphs were constructed from the functional connectivity matrices by including the top 10% of the connections in the graph according to the rank of their correlation strengths (van Wijk et al., 2010; van den Heuvel et al., 2017). This resulted in sparse binary undirected brain graphs at a fixed network density of 10% and assured that the brain graphs were matched in terms of density across participants, resting state, and listening task. Mean functional connectivity was calculated as the average of the upper diagonal elements of the sparse connectivity matrix for each participant. In addition, network modularity was estimated to quantify the configuration of large-scale brain networks on macroscopic level (Rubinov and Sporns, 2010) (Fig. 2A). The mathematical formalization of network modularity is provided in SI Appendix.

Statistical analysis

Behavioral data. Performance of the participants during the listening task was assessed based on a binary measure of correct pitch discrimination (response accuracy: correct/incorrect), the inverse of response time (response speed), and a binary measure of confidence ratings (response confidence: high/low). Trials during which no response was given (within the response time window) and trials on which RT<300ms were excluded. The single-trial behavioral measures across all individual

participants were treated as the dependent variable in the (generalized) linear mixed effects analysis. In models predicting confidence or speed, response accuracy was modeled as a binary predictor.

Brain data. Statistical comparisons of connectivity and network modularity between resting state and listening task were based on permutation tests for paired samples (randomly permuting the rest and task labels 10,000 times). We used Cohen's d for paired samples as the corresponding effect size.

Brain-behavior models. Brain–behavior relationship was investigated within a linear mixed effects analysis framework. To this end, each of the single-trial behavioral measures (response accuracy, speed, or confidence) across all participants was treated as the dependent variable. In models predicting confidence or speed, response accuracy was modeled as a binary predictor. The main predictors in all models were titrated pitch difference (i.e., tracking parameter), time-on-task (i.e., task block number: 1-6), congruency of the tone sequences (congruent vs. not congruent), location of the lateral stream (left vs. right), and the role of the lateral stream (attended vs. ignored). Since in this study, the main question is whether reconfiguration of resting-state brain networks from rest to task relates to listening behavior, we used the mean connectivity or modularity of the brain networks as the main predictors of interest. Specifically, we included the main effect of each rest and task connectivity (or modularity) in the models as between-subject covariates. In addition, to control for activity level of each auditory, cinguloopercular, and dorsal attention network, individual mean beta estimates obtained from activation analysis (Fig. S2) and averaged within each network were similarly included in the models as between-subject covariates.

Deviation coding was used for categorical predictors. All continuous variables were Z scored. Since response accuracy and confidence are binary variables, we used a generalized linear mixed effects model with the logit as link function in these cases. In the case of response speed, the distribution of the data did not significantly deviate from normal distribution (Shapiro–Wilk test P value = 0.8). Thus, in this case, we used linear mixed effects models with the underlying distribution set to Gaussian. For all models predicting response accuracy, confidence or speed, we report P values for individual model terms that were derived using the Satterthwaite approximation for degrees of freedom. All reported p-values are corrected to control for the false discovery rate. As a measure of effects size, for the model predicting accuracy or confidence, we report OR, and for response speed, we report the regression coefficient (β). Mixed effects analyses were performed in R (R Core Team) using the packages lme4 and sjPlot.

Bayes factor. To facilitate the interpretability of significant and non-significant effects, we calculated the Bayes Factor (BF) based on the comparison of Bayesian information criterion (BIC) values as proposed by (Wagenmakers, 2007): BF = exp([BIC(H0)–BIC(H1)]/2). To calculate the BF for a given term, we compared the BIC values of the full model to that of a reduced model in which only the accuracy × interconnectivity interaction term was removed. By convention, log-BFs larger than 1 provide evidence for the presence of an effect (i.e., the observed data are more likely under the more complex model) whereas log-BFs smaller than −1 provide evidence for the absence of an effect (i.e., the observed data are more likely under the simpler or null model) (Dienes, 2014).

Data visualization

Brain surfaces were visualized using Connectome Workbench. Connectograms were visualized using Brain Data Viewer. Network flow diagrams were visualized in MapEquation.

Data availability

The complete dataset associated with this work, including MRI data in BIDS format, and code of network and statistical analyses will be made publicly available upon publication on Open Science platform OSF under the link to the project page https://osf.io/a9cte/.

Acknowledgement

Anne Herrmann helped acquire the fMRI data. The task paradigm had been developed jointly by author M.A. and Malte Wöstmann. Research was supported by German Research Foundation (DFG) - 426620060 (grant to M.A.).

References

Ais J, Zylberberg A, Barttfeld P, Sigman M (2016) Individual consistency in the accuracy and distribution of confidence judgments. Cognition 146:377-386.

Alavash M, Tune S, Obleser J (2019) Modular reconfiguration of an auditory control brain network supports adaptive listening behavior. Proceedings of the National Academy of Sciences of the United States of America 116:660-669.

Alavash M, Tune S, Obleser J (2021) Dynamic large-scale connectivity of intrinsic cortical oscillations supports adaptive listening in challenging conditions. PLoS Biol 19:e3001410.

Alavash M, Hilgetag CC, Thiel CM, Giessing C (2015a) Persistency and flexibility of complex brain networks underlie dual-task interference. Human brain mapping 36:3542-3562.

Alavash M, Doebler P, Holling H, Thiel CM, Giessing C (2015b) Is functional integration of resting state brain networks an unspecific biomarker for working memory performance? NeuroImage 108:182-193.

Alavash M, Daube C, Wöstmann M, Brandmeyer A, Obleser J (2017) Large-scale network dynamics of beta-band oscillations underlie auditory perceptual decision-making. Netw Neurosci 1:166-191.

Alavash M, Lim SJ, Thiel C, Sehm B, Deserno L, Obleser J (2018) Dopaminergic modulation of hemodynamic signal variability and the functional connectome during cognitive performance. NeuroImage 172:341-356.

Arslan S, Ktena SI, Makropoulos A, Robinson EC, Rueckert D, Parisot S (2017) Human brain mapping: A systematic comparison of parcellation methods for the human cerebral cortex. NeuroImage 170:5-30.

Baird B, Smallwood J, Gorgolewski KJ, Margulies DS (2013) Medial and lateral networks in anterior prefrontal cortex support metacognitive ability for memory and perception. The Journal of neuroscience : the official journal of the Society for Neuroscience 33:16657-16665.

Bang D, Fleming SM (2018) Distinct encoding of decision confidence in human medial prefrontal cortex. PNAS.

Barttfeld P, Wicker B, McAleer P, Belin P, Cojan Y, Graziano M, Leiguarda R, Sigman M (2013) Distinct patterns of functional brain connectivity correlate with objective performance and subjective beliefs. Proceedings of the National Academy of Sciences of the United States of America 110:11577-11582.

Bassett DS, Sporns O (2017) Network neuroscience. Nature neuroscience 20:353-364.

Bassett DS, Wymbs NF, Porter MA, Mucha PJ, Carlson JM, Grafton ST (2010) Dynamic reconfiguration of human brain networks during learning. PNAS 108:7641-7646.

Bertolero MA, Yeo BTT, Bassett DS, D'Esposito M (2018) A mechanistic model of connector hubs, modularity and cognition. Nat Hum Behav 2:765-777.

Corbetta M, Patel G, Shulman GL (2008) The reorienting system of the human brain: from environment to theory of mind. Neuron 58:306-324.

Coste CP, Kleinschmidt A (2016) Cingulo-opercular network activity maintains alertness. NeuroImage 128:264-272.

Dai L, Best V, Shinn-Cunningham BG (2018) Sensorineural hearing loss degrades behavioral and physiological measures of human spatial selective auditory attention. Proceedings of the National Academy of Sciences of the United States of America 115:E3286-E3295.

De Martino B, Fleming SM, Garrett N, Dolan RJ (2013) Confidence in value-based choice. Nature neuroscience 16:105-110.

Dosenbach NU, Fair DA, Cohen AL, Schlaggar BL, Petersen SE (2008) A dual-networks architecture of top-down control. Trends in cognitive sciences 12:99-105.

Eckert MA, Teubner-Rhodes S, Vaden KI, Jr. (2016) Is Listening in Noise Worth It? The Neurobiology of Speech Recognition in Challenging Listening Conditions. Ear Hear 37 Suppl 1:101S-110S.

Eckert MA, Menon V, Walczak A, Ahlstrom J, Denslow S, Horwitz A, Dubno JR (2009) At the heart of the ventral attention system: the right anterior insula. Human brain mapping 30:2530-2541.

Erb J, Henry MJ, Eisner F, Obleser J (2013) The brain dynamics of rapid perceptual adaptation to adverse listening conditions. The Journal of neuroscience : the official journal of the Society for Neuroscience 33:10688-10697.

Esteban O, Birman D, Schaer M, Koyejo OO, Poldrack RA, Gorgolewski KJ (2017) MRIQC: Advancing the automatic prediction of image quality in MRI from unseen sites. PLoS One 12:e0184661.

Esteban O, Markiewicz CJ, Blair RW, Moodie CA, Isik AI, Erramuzpe A, Kent JD, Goncalves M, DuPre E, Snyder M, Oya H, Ghosh SS, Wright J, Durnez J, Poldrack RA, Gorgolewski KJ (2019) fMRIPrep: a robust preprocessing pipeline for functional MRI. Nat Methods 16:111-116.

Faskowitz J, Esfahlani FZ, Jo Y, Sporns O, Betzel RF (2020) Edge-centric functional network representations of human cerebral cortex reveal overlapping system-level architecture. Nature neuroscience.

Fleming SM, Dolan RJ (2012) The neural basis of metacognitive ability. Philos Trans R Soc Lond B Biol Sci 367:1338-1349.

Fleming SM, Dolan RJ, Frith CD (2012a) Metacognition: computation, biology and function. Philos Trans R Soc Lond B Biol Sci 367:1280-1286.

Fleming SM, Huijgen J, Dolan RJ (2012b) Prefrontal Contributions to Metacognition in Perceptual Decision Making. The Journal of neuroscience : the official journal of the Society for Neuroscience 32:6117-6125.

Fleming SM, Ryu J, Golfinos JG, Blackmon KE (2014) Domain-specific impairment in metacognitive accuracy following anterior prefrontal lesions. Brain : a journal of neurology 137:2811-2822.

Fleming SM, Weil RS, Nagy Z, Dolan RJ, Rees G (2010) Relating introspective accuracy to individual differences in brain structure. Science 329:1541-1543.

Fox MD, Corbetta M, Snyder AZ, Vincent JL, Raichle ME (2006) Spontaneous neuronal activity distinguishes human dorsal and ventral attention systems. Proceedings of the National Academy of Sciences of the United States of America 103:10046-10051.

Galvin SJ, Podd JV, Drga V, Whitmore J (2003) Type 2 tasks in the theory of signal detectability: discrimination between correct and incorrect decisions. Psychonomic Bull Rev 104:843-876.

Gatehouse S, Noble W (2004) The Speech, Spatial and Qualities of Hearing Scale (SSQ). Int J Audiol 43:85-99.

Geerligs L, Rubinov M, Cam C, Henson RN (2015) State and Trait Components of Functional Connectivity: Individual Differences Vary with Mental State. The Journal of neuroscience : the official journal of the Society for Neuroscience 35:13949-13961.

Gordon EM, Laumann TO, Adeyemo B, Huckins JF, Kelley WM, Petersen SE (2016) Generation and evaluation of a cortical area parcellation from resting-state correlations. Cereb Cortex 26:288-303.

Gordon EM, Lynch CJ, Gratton C, Laumann TO, Gilmore AW, Greene DJ, Ortega M, Nguyen AL, Schlaggar BL, Petersen SE, Dosenbach NUF, Nelson SM (2018) Three distinct sets of connector hubs integrate human brain function. Cell Rep 24:1687-1695 e1684.

Gorgolewski KJ et al. (2016) The brain imaging data structure, a format for organizing and describing outputs of neuroimaging experiments. Sci Data 3:160044.

Gratton C, Sun H, Petersen SE (2017) Control networks and hubs. Psychophysiology.

Gratton C, Laumann TO, Nielsen AN, Greene DJ, Gordon EM, Gilmore AW, Nelson SM, Coalson RS, Snyder AZ, Schlaggar BL, Dosenbach NUF, Petersen SE (2018) Functional brain networks are dominated by stable group and individual factors, not cognitive or daily Variation. Neuron 98:439-452 e435.

Guggenmos M (2021) Measuring metacognitive performance: type 1 performance dependence and test-retest reliability. Neurosci Conscious 2021:niab040.

Halchenko YOea (2018) Open Source Software: Heudiconv. Zenodo.

Hebart MN, Schriever Y, Donner TH, Haynes JD (2016) The Relationship between Perceptual Decision Variables and Confidence in the Human Brain. Cereb Cortex 26:118-130.

Hill KT, Miller LM (2010) Auditory attentional control and selection during cocktail party listening. Cereb Cortex 20:583-590.

Kayser SJ, McNair SW, Kayser C (2016) Prestimulus influences on auditory perception from sensory representations and decision processes. PNAS 113:4842-4847.

Kepecs A, Uchida N, Zariwala HA, Mainen ZF (2008) Neural correlates, computation and behavioural impact of decision confidence. Nature 455:227-231.

Kiani R, Shadlen MN (2009) Representation of confidence associated with a decision by neurons in the parietal cortex. . Science 324:759-764.

Lee AK, Larson E, Maddox RK, Shinn-Cunningham BG (2014) Using neuroimaging to understand the cortical mechanisms of auditory selective attention. Hearing research 307:111-120.

Marek S, Dosenbach NUF (2018) The frontoparietal network: function, electrophysiology, and importance of individual precision mapping. Dialogues Clin Neurosci 20:133-140.

Menon V, Uddin LQ (2010) Saliency, switching, attention and control: a network model of insula function. Brain Struct Funct 214:655-667.

Menon V, D'Esposito M (2022) The role of PFC networks in cognitive control and executive function. Neuropsychopharmacology 47:90-103.

Middlebrooks PG, Sommer MA (2012) Neuronal correlates of metacognition in primate frontal cortex. Neuron 75:517-530.
Murphy K, Fox MD (2016) Towards a consensus regarding global signal regression for resting state functional connectivity MRI. NeuroImage 154:169-173.
Neta M, Schlaggar BL, Petersen SE (2014) Separable responses to error, ambiguity, and reaction time in cingulo-opercular task control regions. NeuroImage 99:59-68.
Neta M, Nelson SM, Petersen SE (2017) Dorsal Anterior Cingulate, Medial Superior Frontal Cortex, and Anterior Insula Show Performance Reporting-Related Late Task Control Signals. Cereb Cortex 27:2154-2165.
Oldfield R (1971) The assessment and analysis of handedness: The Edinburgh inventory. Neuropsychologia 9:97-113.
Palmer EC, David AS, Fleming SM (2014) Effects of age on metacognitive efficiency. Conscious Cogn 28:151-160.
Parkes L, Fulcher B, Yucel M, Fornito A (2018) An evaluation of the efficacy, reliability, and sensitivity of motion correction strategies for resting-state functional MRI. NeuroImage 171:415-436.
Peelle JE (2017) Listening Effort: How the Cognitive Consequences of Acoustic Challenge Are Reflected in Brain and Behavior. Ear Hear.
Petersen SE, Posner MI (2012) The attention system of the human brain: 20 years after. Annu Rev Neurosci 35:73-89.
Posner MI (2012) Imaging attention networks. NeuroImage 61:450-456.
Power JD, Petersen SE (2013) Control-related systems in the human brain. Current opinion in neurobiology 23:223-228.
Power JD, Plitt M, Laumann TO, Martin A (2017) Sources and implications of whole-brain fMRI signals in humans. NeuroImage 146:609-625.
Power JD, Cohen AL, Nelson SM, Wig GS, Barnes KA, Church JA, Vogel AC, Laumann TO, Miezin FM, Schlaggar BL, Petersen SE (2011) Functional network organization of the human brain. Neuron 72:665-678.
Puschmann S, Steinkamp S, Gillich I, Mirkovic B, Debener S, Thiel CM (2017) The right temporoparietal junction supports speech tracking during selective listening: Evidence from concurrent EEG-fMRI. The Journal of neuroscience : the official journal of the Society for Neuroscience 37:11505-11516.
Rouault M, Lebreton M, Pessiglione M (2023) A shared brain system forming confidence judgment across cognitive domains. Cereb Cortex 33:1426-1439.
Rouault M, McWilliams A, Allen MG, Fleming SM (2018) Human metacognition across domains: insights from individual differences and neuroimaging. Personal Neurosci 1.
Rubinov M, Sporns O (2010) Complex network measures of brain connectivity: uses and interpretations. NeuroImage 52:1059-1069.
Sadaghiani S, D'Esposito M (2015) Functional Characterization of the Cingulo-Opercular Network in the Maintenance of Tonic Alertness. Cereb Cortex 25:2763-2773.
Sadaghiani S, Kleinschmidt A (2016) Brain Networks and alpha-Oscillations: Structural and Functional Foundations of Cognitive Control. Trends in cognitive sciences 20:805-817.
Seeley WW, Menon V, Schatzberg AF, Keller J, Glover GH, Kenna H, Reiss AL, Greicius MD (2007) Dissociable intrinsic connectivity networks for salience processing and executive control. The Journal of neuroscience : the official journal of the Society for Neuroscience 27:2349-2356.
Sestieri C, Corbetta M, Spadone S, Romani GL, Shulman GL (2014) Domain-general signals in the cingulo-opercular network for visuospatial attention and episodic memory. Journal of cognitive neuroscience 26:551-568.
Shiell MM, Hausfeld L, Formisano E (2018) Activity in Human Auditory Cortex Represents Spatial Separation Between Concurrent Sounds. The Journal of neuroscience : the official journal of the Society for Neuroscience 38:4977-4984.
Shinn-Cunningham B (2017) Cortical and Sensory Causes of Individual Differences in Selective Attention Ability Among Listeners With Normal Hearing Thresholds. J Speech Lang Hear Res 60:2976-2988.
Shinn-Cunningham BG (2008) Object-based auditory and visual attention. Trends in cognitive sciences 12:182-186.
Szczepanski SM, Pinsk MA, Douglas MM, Kastner S, Saalmann yB (2013) Functional and structural architecture of the human dorsal frontoparietal attention network. PNAS 110:15806-15811.
Tune S, Alavash M, Fiedler L, Obleser J (2021) Neural attentional-filter mechanisms of listening success in middle-aged and older individuals. Nat Commun 12:4533.
Uddin LQ (2015) Salience processing and insular cortical function and dysfunction. Nature reviews Neuroscience 16:55-61.
Vaccaro AG, Fleming SM (2018) Thinking about thinking: A coordinate-based meta-analysis of neuroimaging studies of metacognitive judgements. Brain Neurosci Adv 2:2398212818810591.
Vaden KI, Jr., Eckert MA, Dubno JR, Harris KC (2019) Cingulo-opercular adaptive control for younger and older adults during a challenging gap detection task. J Neurosci Res.

Vaden KI, Jr., Teubner-Rhodes S, Ahlstrom JB, Dubno JR, Eckert MA (2022) Evidence for cortical adjustments to perceptual decision criteria during word recognition in noise. NeuroImage 253:119042.

Vaden KI, Jr., Kuchinsky SE, Cute SL, Ahlstrom JB, Dubno JR, Eckert MA (2013) The cingulo-opercular network provides word-recognition benefit. The Journal of neuroscience : the official journal of the Society for Neuroscience 33:18979-18986.

van den Heuvel M, de Lange S, Zalesky A, Seguin C, Yeo T, Schmidt R (2017) Proportional thresholding in resting-state fMRI functional connectivity networks and consequences for patient-control connectome studies: Issues and recommendations. NeuroImage 152:437-449.

van Wijk BCM, Stam CJ, Daffertshofer A (2010) Comparing Brain Networks of Different Size and Connectivity Density Using Graph Theory. PloS one 5:e13701.

Vossel S, Geng JJ, Fink GR (2014) Dorsal and ventral attention systems: distinct neural circuits but collaborative roles. The Neuroscientist : a review journal bringing neurobiology, neurology and psychiatry 20:150-159.

Walker EY, Pohl S, Denison RN, Barack DL, Lee J, Block N, Ma WJ, Meyniel F (2023) Studying the neural representations of uncertainty. Nature neuroscience.

Waschke L, Wostmann M, Obleser J (2017) States and traits of neural irregularity in the age-varying human brain. Sci Rep 7:17381.

Waters F, Allen P, Aleman A, Fernyhough C, Woodward TS, Badcock JC, Barkus E, Johns L, Varese F, Menon M, Vercammen A, Laroi F (2012) Auditory hallucinations in schizophrenia and nonschizophrenia populations: a review and integrated model of cognitive mechanisms. Schizophrenia bulletin 38:683-693.

Wild CJ, Yusuf A, Wilson DE, Peelle JE, Davis MH, Johnsrude IS (2012) Effortful listening: the processing of degraded speech depends critically on attention. The Journal of neuroscience : the official journal of the Society for Neuroscience 32:14010-14021.

Wostmann M, Waschke L, Obleser J (2019) Prestimulus neural alpha power predicts confidence in discriminating identical auditory stimuli. Eur J Neurosci 49:94-105.

Wostmann M, Erb J, Kreitewolf J, Obleser J (2021) Personality captures dissociations of subjective versus objective hearing in noise. R Soc Open Sci 8:210881.

Wöstmann M, Alavash M, Obleser J (2019) Alpha Oscillations in the Human Brain Implement Distractor Suppression Independent of Target Selection. The Journal of neuroscience : the official journal of the Society for Neuroscience 39:9797-9805.

Zhang Z, Telesford QK, Giusti C, Lim KO, Bassett DS (2016) Choosing Wavelet Methods, Filters, and Lengths for Functional Brain Network Construction. PloS one 11:e0157243.